Analysis of endgas temperature fluctuations in an SI engine by laser–induced fluorescence

R. Schießl [a] U. Maas [a]

[a] *Institut für Technische Verbrennung, Pfaffenwaldring 12, D–70 569 Stuttgart*

Abstract

We investigate spatial temperature fluctuations in the unburned endgas of a spark–ignited (SI) engine. Our approach exploits the fact that the quantities (species concentrations, temperature) comprising the state of the combustion chamber gases are not *independent*, but often *correlate* sharply. Information about spatial temperature variations is obtained indirectly by observing two complementary quantities that sensitively reflect the local temperature. Spatial formaldehyde (H_2CO) concentration variations in the endgas are converted to temperature fluctuations using calculated correlations between temperature and $[H_2CO]$. Additionally, the geometrical size of inhomogeneities is deduced from LIF–images displaying the locally varying formation of temperature–sensitive intermediate species.

The results indicate that temperature fluctuations exceeding 20 K are present in the *nominally* homogeneous endgas. The geometrical size of these fluctuations ranges from ≈1 mm to ≈1 cm.

Key words: IC engines, endgas, temperature fluctuations, laser–induced fluorescence

1 Introduction

Spatial temperature fluctuations in the cylinder gases of SI engines can be of deep impact on the combustion process. For instance, it is known that sites of locally increased temperature in the endgas can lead to engine knock [1]. Numerical calculations have shown that even very *small* temperature fluctuations in the order of 10 K may have *large* influence on the onset of auto–ignition [2–4]. Detailed experimental studies show the strong influence of temperature on chemical kinetics and ignition behaviour of alkane/air mixtures [5].

Currently, however, there is no direct measurement strategy available that could detect such tiny, instationary temperature fluctuations in an operating engine. The known techniques for direct, time resolved temperature measurement in instationary gas flows such as LIF [6], Rayleigh scattering [7], and CARS [8,9] suffer from limited applicability or accuracy when they should be utilised for two–dimensional temperature measurements in the combustion chamber of an engine. Additionally, some require doping the fuel with a tracer, which may affect the behaviour of the system under investigation.

However, with laser based techniques, it is often possible to obtain detailed and accurate information about some processes and quantities in the endgas that are *strongly dependent* on temperature. Such quantities are the formation or consumption of certain species like formaldehyde and other intermediates that are involved in strongly temperature dependent reactions.

Email addresses: schiessl@itv.uni-stuttgart.de (R. Schießl),
maas@itv.uni-stuttgart.de (U. Maas).
URL: http://www.uni-stuttgart.de/itv/ (U. Maas).

The aim of this work is, consequently, to combine the results of LIF–measurements in an engine with detailed calculations of chemical kinetics in order to estimate temperature fluctuations in the endgas. For this purpose, measured planar maps of intermediate species concentrations and one–dimensional profiles of formaldehyde (H_2CO) are analysed based on information from modelling calculations.

2 Experimental setup

2.1 Engine

All investigations were performed on an experimental two–stroke engine based on an ILO L372 crankcase and cylinder [10]. The cylinder head was equipped with glass windows to allow optical access into the combustion chamber; figure 1 sketches details of the design. The engine was operated was at 1000 rpm with blends of iso–octane and n–heptane (PRF 90). To minimise the amount of burned gases trapped inside cylinder, the engine was skip–fired: Only every 5^{th} cycle was ignited, while fresh fuel/air mixture was scavenged through the combustion chamber in the remaining 4 cycles. This ensured well defined in–cylinder conditions at BDC, such alleviating comparison of measurements with numerical calculations. To guarantee a constant engine speed, the crankshaft was coupled to a dynamometer (Siemens SIMODRIVE) and equipped with a large–dimensioned flywheel (moment of inertia 0.216 kg·m^2). Table 1 lists additional engine specifications.

Fig. 1

Tab. 1

2.2 LIF visualisation of intermediate species

For imaging the occurrence of intermediate species, a double–pulse LIF set–up as shown in figure 2 was used. As explained in [11], the experiment delivers a pair of subsequently recorded LIF–images from the same engine cycle. In these images, locations where intermediate species are present in the endgas are visible by their bright fluorescence. In contrast, regions without intermediates appear dark. In ignited regions ("hot–spots"), intermediates are consumed very rapidly; these sites therefore show up as dark spots on the bright fluorescent background. Correspondingly, regions that display a too low temperature to allow intermediates to be formed, also appear dark.

This experimental scheme is similar to the one presented in [12], but relies on the detection of intermediate species excited at 308 nm, instead of formaldehyde excitation at 353 nm. Our excitation strategy has the advantage that it delivers strong fluorescence signals, resulting in images of good signal–to–noise ratio. However, in contrast to excitation of the endgas at 353 nm, at 308 nm the fluorescing species cannot be identified uniquely. It is known that many intermediates are present in the endgas during the late compression phase, especially ketones and aldehydes that display fluorescence after irradiation at 308 nm [13,14].

The pulsed radiation (pulse width 20 ns, energy $\approx$ 200 mJ per pulse) of two XeCl–excimer lasers (Lambda Physik LPX 205) was formed into light sheets of $\approx 500\,\mu$m thickness, and a width of ≈ 5 cm. They were shone into the combustion chamber of the engine. For each laser, one intensified CCD camera (Proxitronic NANOCAM, dynamic range 8 bit, 512×512 pixels) was employed Fig. 2

to capture the fluorescence signal out of the combustion chamber. Triggering each laser–camera system independently at prescribed crank angles by a crank–angle encoder and delay generators allowed us to capture a sequence of two LIF–images with adjustable delay between the images. For every image pair, the corresponding in–cylinder pressure trace was recorded with a piezoelectric transducer (Kistler 6001) at a scan rate of 2 scans per crank angle.

The images and pressure traces were digitised and stored on a PC for later analysis. A more detailed description of the set–up can be found in [11].

2.3 LIF–Measurement of formaldehyde concentrations

For the visualisation of formaldehyde in the endgas, a detection of fluorescence intensity along a line was used; details of the experimental scheme are outlined in [15]. The $2_0^1 4_0^1$ vibrational band of the A^1A_2—X^1A_1 electronic transition of H_2CO was excited with a pulsed, XeCl–excimer pumped dye laser at 339.3 nm. By recording the fluorescence emission spectrum resulting from laser excitation of the endgas, it was assured that formaldehyde was the only fluorescence emitter. Although the set–up is designed to allow spatially resolved measurements of formaldehyde concentrations along a line on a single–shot basis [15], only information about spatial *relative fluctuations* is needed within the scope of this paper (see below).

3 Results and Discussion

Using the set–ups described above allows us to perform two complementary measurements: Two dimensional imaging of intermediate species in the endgas

and line imaging of formaldehyde concentrations. The first one delivers detailed spatial information about the endgas, without identifying the chemical species under investigation. The latter delivers one dimensional concentration profiles of formaldehyde.

In the following sections, the results of these measurements will be presented and their relevance for detecting temperature fluctuations will be discussed.

3.1 LIF of intermediate species

Figure 3 shows a typical LIF image pair obtained with the double–pulse set–up from fig. 2. It was recorded during a knocking engine cycle at 13° CAD ATDC, with a delay between the images of 101 μs. The absence of fluorescing intermediate species due to ignition is seen in both the regular flame and self–igniting centers. While the regular flame hardly shows any change, the self–igniting centers expand considerably in this short time span. This observation is in agreement with the results of Bäuerle et al. [12], who used formaldehyde for the detection of auto–igniting centers in the same engine.

Fig: 3

In figure 4 an image pair is shown that was recorded in cycle of relatively low cylinder pressure, in a non–knocking cycle. Here, dark sites are visible as well, but they do not, as opposed to "hot–spots", have large expansion velocities, nor are they accompanied by the steep pressure rise that is always observed when auto–ignition occurs in the endgas. The pockets can not be due to inhomogeneous fuel/air mixture distribution. Our engine features external carburation along with crank–case scavenging, and the mixture distribution is very homogeneous, as has been confirmed clearly by fuel–tracer LIF approaches.

The dark pockets are sites of lower temperature, where intermediates have not yet formed. Fig:4

It is known that the formation of intermediates is a highly temperature sensitive process; therefore, temperature variations are displayed as fluctuations in intermediate concentration fields. It can therefore be assumed that the detected fluorescence signal at each location within one LIF–trace is proportional to the local number density. To investigate how information about temperature fluctuations can be gathered from these images, it is necessary to investigate the calculated correlation between temperature and concentrations [mol/m^3] of intermediate species, as depicted for the example of acetone (C_2H_6O) and acetaldehyde (CH_3CHO) in fig. 5. These correlations display the qualitative behaviour of intermediates in dependence of temperature; also, different phases of the evolution process from unburned gases to burned gases are visible. In this section, the analysis is purely *qualitative*. The exact identification of the fluorescent intermediates is therefore not necessary, as all intermediates follow the same qualitative picture of formation/consumption during the compression phase prior to ignition.

The correlations were obtained by homogeneous reactor calculations [16] with experimental cylinder pressure traces $p(t)$ as external constraint. Calculations were performed for initial gas temperatures varying in a range from 300 K to 380 K; this was of no noticeable effect on the resulting correlation curves. The chemical kinetics was described by a detailed iso–octane/n–heptane mechanism specially developed for low–temperature kinetics and therefore accounting various effects like a negative temperature coefficient of ignition delay time, and endo— or exothermic reactions before ignition. [15]. The engine cycle starts at low temperatures (left–most part of the correlation curves), where Fig: 5

no intermediate species are present. As the piston and regular flame front compress the endgas, the temperature increases, (corresponding to a motion from left to right), and intermediate concentrations increase monotonically in a wide temperature range. At a certain point, a maximum is reached, and afterwards concentrations decay as the system moves into higher temperature ranges, finally leading to auto–ignition (rightmost side).

All intermediates display the same qualitative behaviour during an engine cycle:

- During the compression phase, their mole fraction (and concentration) increases with temperature. Intermediate species mole fractions display a highly nonlinear, strong Arrhenius–like temperature dependence. For this part of the engine cycle, the intermediate species concentrations rise monotonically with temperature.
- After reaching the culmination point, intermediates are consumed and disappear quickly. In this phase, temperature rise is mainly due to chemical reaction; there is not necessarily a monotonic dependence between intermediate concentration and temperature. Reaching the right branch will, eventually, lead to auto—ignition.

Therefore, despite the fact that the species causing the fluorescence in our images is (or are) not uniquely identified, charts like the one depicted in fig. 6 can be used to display the qualitative behaviour of the endgas. The dark pockets seen in images where the engine was "cold", i. e., where the compression started at a lower mixture temperature due to absence of heating by hot crankcase walls (fig. 4) correspond to the leftmost side of the correlation curve; the brighter regions in these images are located in a state of slightly

Fig: 6

higher temperature, corresponding to the monotonically increasing part of the curve. The fact that in these cycles no auto–ignition was observed guarantees that the right part of the correlation curve is not reached by the system. At a regular engine cycle (no auto–ignition), the state is located at higher temperatures, but still the region right to the maximum is never reached. In knocking cycles, the dark spots clearly correspond to the rightmost region, where intermediates have been consumed by the reactions leading to ignition. Endgas regions that do not display self–ignition in the first image of the measured sequence, but ignite immediately afterwards (as visible in the second image) can be attributed to the right branch of the correlation curve.

Previous experiments have shown that the endgas does not display *large* inhomogeneities in temperature or major species concentration[6]; we therefore observe *small* fluctuations. Consequently, the variation of temperature or composition dependent contributions to the fluorescence efficiency (like thermal population of the probed molecular ground state, collisional quenching rates, etc.) can be neglected in our case. The assumption that the local LIF intensity increases monotonically with the local concentration of the fluorescing species is then valid.

The measured LIF–images, therefore, contain information about spatial temperature fluctuations. Although this information is only qualitative with respect to the magnitude of the temperature fluctuations, it allows a quantitative estimation of the geometrical size distribution of temperature fluctuations. This is important for characterising the turbulent scales present in the combustion chamber.

By measuring the sizes of “cool spots” for a large number of images using

simple image processing techniques, the typical scale of these fluctuations can be determined. In our case, size ranges from 1 mm to 1 cm have been deduced.

3.2 LIF of formaldehyde

A strong correlation with temperature is also found for the concentration of formaldehyde, as shown in fig. 7. This indicates possibilities of detecting temperature fluctuations by means of measuring spatial changes in $[H_2CO]$. Variations of temperature are mapped directly onto variations of formaldehyde, via the relationship $[H_2CO] \approx f(T)$. Because formaldehyde is an intermediate species, the considerations from section 3.1 apply. The advantage of formaldehyde is that it can be detected without interference of other species. As mentioned in the experimental section, this was carefully checked in our experiments by recording the fluorescence emission spectrum from the endgas. To obtain temperature fluctuations, *relative* fluctuations of $[H_2CO]$ have to be determined from the variations in LIF–Intensities (see below). This procedure does not require explicit knowledge about absolute values of quenching efficiency, predissociation rates, population of the laser-exited ground state or fluorescence trapping. It merely requires knowledge about *relative variation* of these quantities with temperature. Using vibrational frequencies and rotational constants of the formaldehyde molecule of [17], we calculated the change of thermal population for rotational energy levels by the program WANG (D. Luckhaus, ETH Zuerich, 2000) [18] and for the vibronic ground state in the probed $4_0^1 2_0^1$ vibrational band near 339 nm. In the relevant temperature range (700 K—1000 K), the temperature–induced variation of ground state population is by a factor of more than 6 smaller than the variation of formaldehyde

number density. With the homogeneous mixture in our engine, variations of quenching due to local changes in chemical composition are negligible. Assuming a $\sqrt{T}$ dependence of fluorescence quenching efficiency, the variation of quenching with temperature is 20 times weaker than the corresponding change of [H_2CO]. Fluorescence trapping is no issue in our experiment due to the short path (2 mm) the fluorescence light has to travel through the endgas, and the weak absorption of formaldehyde in the wavelength range of the fluorescence emission. Therefore, the fluorescence signal at different locations in the endgas is, to a good approximation, proportional to the local formaldehyde concentration. The proportionality factor may vary largely between different engine cycles, but this does in no way affect our method that mereley compares intensities from one LIF trace. A quantitative determination of temperature inhomogeneities from variation of formaldehyde number densities is possible by means the following considerations. In the temperature range present during our measurements (well below the knock–limit), numerical calculations reveal an almost linear dependence between the logarithm of formaldehyde number density [H_2CO] and temperature (see fig. 7, right picture):

$$\log[\mathrm{H_2CO}] \approx A + BT \qquad . \tag{1}$$

Due to the linear relationship $\log[\mathrm{H_2CO}](T)$,

$$\frac{\Delta \log[\mathrm{H_2CO}]}{\Delta T} \approx \frac{\mathrm{d} \log[\mathrm{H_2CO}]}{\mathrm{d}T} \approx B \tag{2}$$

for deviations $\Delta \log[\mathrm{H_2CO}]$ and ΔT of formaldehyde concentrations and temperatures, respectively. B is the slope of the $\log[\mathrm{H_2CO}](T)$ curve and is known from calculations (see figure 7).

From measured one–dimensional traces of $[H_2CO]$ like the one depicted in figure 8, the fluctuation in $[H_2CO]$ can be deduced, and a relative variance $\Delta_{\mathrm{rel.}}H_2CO$ can be determined by

$$\Delta_{\mathrm{rel.}}[H_2CO] = \frac{\sqrt{\overline{\left([H_2CO] - \overline{[H_2CO]}\right)^2}}}{\overline{[H_2CO]}}. \tag{3}$$

Fig: 8

By measuring this quantity in 32 formaldehyde traces for each crank angle, it is seen that the formaldehyde concentration displays considerable local deviation from the spatial mean value, $\overline{[H_2CO]}$. For crank angles in the range $0 \ldots 20$ CAD ATDC, these relative fluctuations are in the range of $\pm 15\%$. Note that this value is not due to measurement noise, but reflects the large–scale variations of $[H_2CO]$ measured in the endgas. The signal fluctuation induced by noise from the camera was checked by recording the fluorescence trace from a homogeneously distributed tracer in a measurement cell; it is very small, as can be seen also from the camera signal obtained in the burned region (fig. 8), and can be neglected.

The right side of fig. 7 demonstrates how this fluctuation amplitude in concentration is mapped onto a temperature interval via the correlation $[H_2CO] = f(T)$. Note that in the right chart of fig. 7, concentration is plotted in a logarithmic scale (according to eq. 1); therefore, an interval corresponding to a certain deviation $[\overline{[H_2CO]}/x \ldots \overline{[H_2CO]} \cdot x], x > 1$ from a mean value $\overline{[H_2CO]}$ appears as an interval of constant width $2 \cdot \log x$ on the chart, regardless of the actual value of $\overline{[H_2CO]}$. From this chart, $\Delta T \approx 20\,\mathrm{K}$ is derived, in a large temperature range almost independently of the mean value $\overline{[H_2CO]}$, where the relative variance is applied. It has, however, to be noted that this procedure is valid only if the system is on the left branch of the H_2CO–T correlation curve

Fig: 7

at the time of measurement. Especially, the method is certainly invalid after auto–ignition has occured.

4 Conclusions

Using calculated correlations between intermediate species and temperature, we have applied two methods for visualising and estimating spatial temperature fluctuations in the endgas of an Otto engine. The methods are based on the observation that pronounced LIF intensity fluctuations of intermediate species are found in the endgas that can not be attributed to mixture distribution inhomogeneities. From fluctuations in two–dimensional intermediate species concentration fields measured with LIF, information about the distribution and the geometrical size of temperature deviations is derived; spatial fluctuations of measured one–dimensional formaldehyde profiles are used for a quantitative estimation of the amplitude of the deviations.

Qualitatively, in the *nominally* homogeneous endgas, considerable temperature fluctuations are present, which is evident from the well known fact that auto–ignition in engines typically happens at a few localised sites of increased temperature, the "hot–spots". This paper is a step towards a quantitative characterisation of these temperature fluctuations. For the engine used in this work we observed that fluctuations are mainly of large–scale in the spatial dimension, with scales typically in the range of 1 mm to 1 cm. Quantitatively, the temperature variations are considerable in their amplitude: The observed formaldehyde signals variations indicate that fluctuations exceeding 20 K are present.

The presented methods display a tool for characterising small temperature fluctuations. They are applicable in reaction systems with a nearly homogeneous mixture distribution and in a temperature range where intermediates like formaldehyde are formed. They offer a remarkable sensitivity combined with high temporal and spatial resolution.

Acknowledgements

The authors are grateful to David Luckhaus from the Institut für Physikalische Chemie, Universität Göttingen, for kindly granting a copy of his program WANG and for his advice in using it; the support of Thomas Dreier and Peter Radi (ETH Zürich) is gratefully acknowledged.

Abbreviations

ATDC	After top dead center
BDC	Bottom dead center
BTDC	Before top dead center
CAD	Crank angle degree
CCD	Charge coupled device
LIF	Laser-induced fluorescence
PRF	Primary reference fuel
TDC	Top dead center

References

[1] A. K. Oppenheim. The knock syndrome — Its cures and its victims. In *SAE Transactions*, volume 93, paper no. 841339, section 5, pages 874–883. Society of Automotive Engineers, 1984.

[2] G. Goyal, U. Maas, and J. Warnatz. Numerical Study of Hot Spot Ignition in H_2-O_2 and CH_4-air mixtures. In *23*rd *Symposium (International) on Combustion*, page 1767. The Combustion Institute, Pittsburgh, PA, 1990.

[3] A. Dreizler and U. Maas. Influence of the temperature distribution on the auto-ignition in the endgas of Otto engines. In *Proc. COMMODIA 1998*. The Japanese Society of Mechanical Engineers, 1998.

[4] S. Hajireza, F. Mauss, and Bengt Sundén. Hot–Spot autoignition in spark ignition engines. *Proceedings of the Combustion Institute*, 28:1169–1175, 2000.

[5] A. Cox, J. Griffiths, C. Mohamed, H. J. Curran, W. J. Pitz, and C. K. Westbrook. Extents of alkane combustion during rapid compression leading to single and two–stage ignition. *26th Symposium (International) on Combustion/The Combustion Institute*, pages 2685–2692, 1996.

[6] S. Einecke, C. Schulz, V. Sick, R. Schießl, A. Dreizler, and U. Maas. Two-dimensional temperature measurements in the compression stroke of an SI engine using two-line tracer LIF. In *SAE paper series No. 982468*. Society of Automotive Engineers, 1998.

[7] C. Schulz, V. Sick, J. Wolfrum, V. Drewes, M. Zahn, and R. Maly. Quantitative 2D single-shot imaging of NO concentrations and temperatures in a transparent SI engine. *Proc. Combust. Inst. 26*, pages 2597–2604, 1996.

[8] R. P. Lucht, D. Dunn-Rankin, T. Walter, T. Dreier, and S. C. Bopp. Heat transfer in engines: Comparison of CARS thermal boundary layer measurements and heat flux measurements. *SAE 910722*, 1991.

[9] J. Bood, P.-E. Bengtsson, F.Mauss, K. Burgdorf, and I. Denbratt. Knock in Spark-Ignition Engines: End–Gas Temperature Measurements Using Rotational CARS and Detailed Kinetic Calculations of the Autoignition. *SAE 971669*, 1997.

[10] B. Bäuerle, F. Hoffmann, F. Behrendt, and J. Warnatz. Detection of hot-spots in the end-gas of an internal combustion engine using two-dimensional LIF of formaldehyde. *25th Symposium (International) on Combustion/The Combustion Institute*, pages 135–141, 1994.

[11] R. Schießl, A. Dreizler, U. Maas, J. Grant, and P. Ewart. Double-Pulse PLIF imaging of self–ignition centers in an SI engine. *SAE technical paper series*,

2001. no. 2001–01–1925.

[12] B. Bäuerle, J. Warnatz, and F. Behrendt. Time resolved investigation of hot spots in the end gas of an S.I. engine by means of2-D double pulse LIF of formaldehyde. *26th Symposium (International) on Combustion/The Combustion Institute*, pages 2619–2626, 1996.

[13] W. W. Simons, editor. Sadtler research laboratories, 1979.

[14] G. Herzberg. *Molecular spectra and molecular structure*, volume III. Krieger Publishing Company, reprint edition, 1991. p. 543, ISBN 0–89464–270–7.

[15] R. Schießl, P. Pixner, A. Dreizler, and U. Maas. Formaldehyde formation in the endgas of Otto engines: Numerical simulations and quantitative concentration measurements. *Combustion Science and Technology*, 149:339–360, 1999.

[16] U. Maas, B. Raffel, J. Wolfrum, and J. Warnatz. Observation and Simulation of Laser Induced Ignition Processes in $O_2 - O_3$ and $H_2 - O_2$-Mixtures. In *21*st *Symposium (International) on Combustion*, page 1869. The Combustion Institute, Pittsburgh, PA, 1986.

[17] J. Clouthier D. and A. Ramsay D.˙ The spectroscopy of Formaldehyde and Thioformaldehyde. *Ann. Rev. Phys. Chem.*, 34:31—58, 1983.

[18] D. Luckhaus and M. Quack. *Mol. Phys.*, 68(3):745—758, 1989.

Tables

Table 1:

Data of the experimental engine

Table 1

make	modified ILO L372
type	two–stroke, single–cylinder, spark ignited
bore	80 mm
stroke	74 mm
displacement	372 cm^3
speed	1000 rpm
compression ratio	approx. 8.5
mixture formation	carburettor BING DRC
fuel	iso–octane/n–heptane primary reference fuel (90%/10% vol./vol.)
spark timing	23° CAD BTDC
equivalence ratio Φ ...	1 ± 0.1

Figures

Figure 1:

Sketch of the optically accessible two–stroke engine used for our measurements.

Figure 2:

Experimental setup for the double–pulse LIF imaging of auto–ignition centers in the engine.

Figure 3:

Example of a LIF image pair of a knocking cycle. The first image was captured at 13 CAD ATDC, the delay between the images is 100 μs.

Figure 4:

Image sequence showing regions ("dark spots") in the endgas where intermediate species have not formed. The delay between the images is 100 μs; the right image appears darker due to the lower pump laser energy and lower collection efficiency of the applied optical line.

Figure 5:

Calculated correlation (for engine conditions) between temperature and the concentration of two important intermediate species in hydrocarbon combus-

tion: acetone ($2C_3H_6O$) and acetaldehyde (C_3H_6O). Shown are the results for different measured engine pressure traces used as temporal conditions for the calculations.

Figure 6:

Chart of different thermokinetic states of the endgas and their correspondence to LIF–images.

Figure 7:

Left: correlation between formaldehyde concentration and temperature, calculated for engine conditions. Each trace corresponds to a measured pressure trace used as input to the calculation. Right: the same correlation, shown in a smaller temperature range and a logarithmic concentration scale. The horizontal bars denote a variance of $\pm 15\%$ around different mean values $[\overline{H_2CO}]$.

Figure 8:

Single–shot 1D–profile of formaldehyde concentration in the endgas.

Fig. 1.

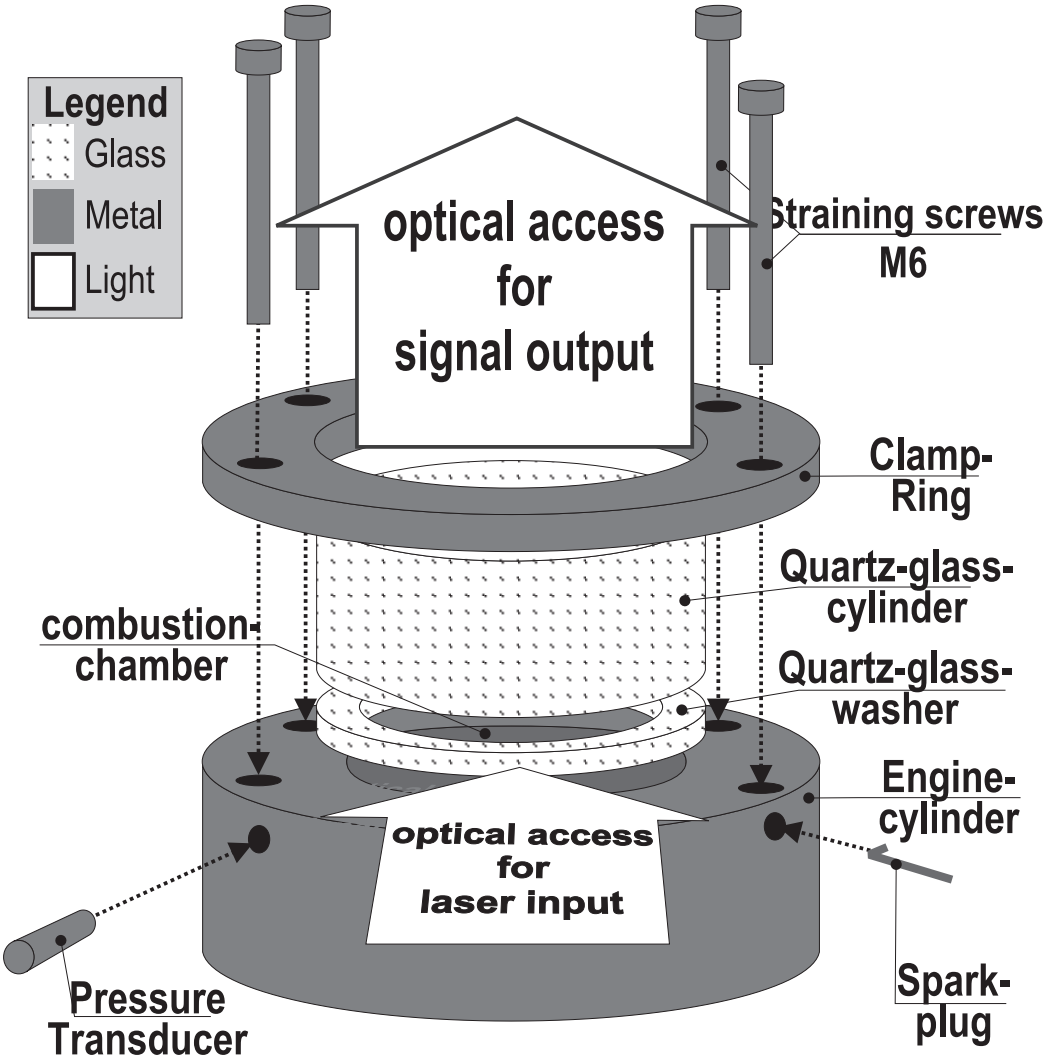
Legend
Glass
Metal
Light
optical access for signal output
Straining screws M6
Clamp-Ring
Quartz-glass-cylinder
combustion-chamber
Quartz-glass-washer
Engine-cylinder
optical access for laser input
Pressure Transducer
Spark-plug

Fig. 2.

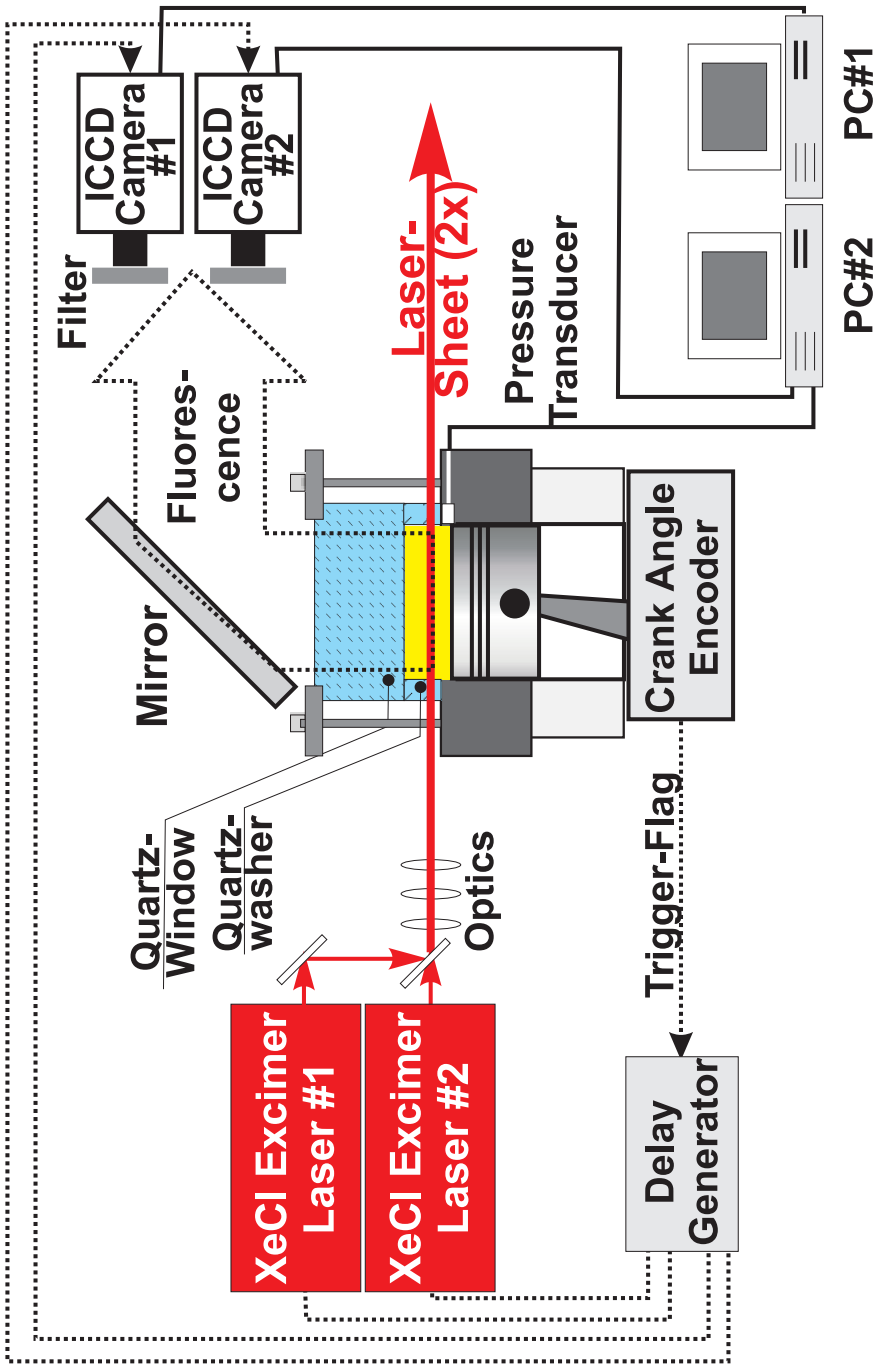
ICCD Camera #1
ICCD Camera #2
Filter
Fluores-cence
Laser-Sheet (2x)
Pressure Transducer
PC#1
PC#2
Mirror
Crank Angle Encoder
Quartz-Window
Quartz-washer
Optics
Trigger-Flag
XeCl Excimer Laser #1
XeCl Excimer Laser #2
Delay Generator

Fig. 3.

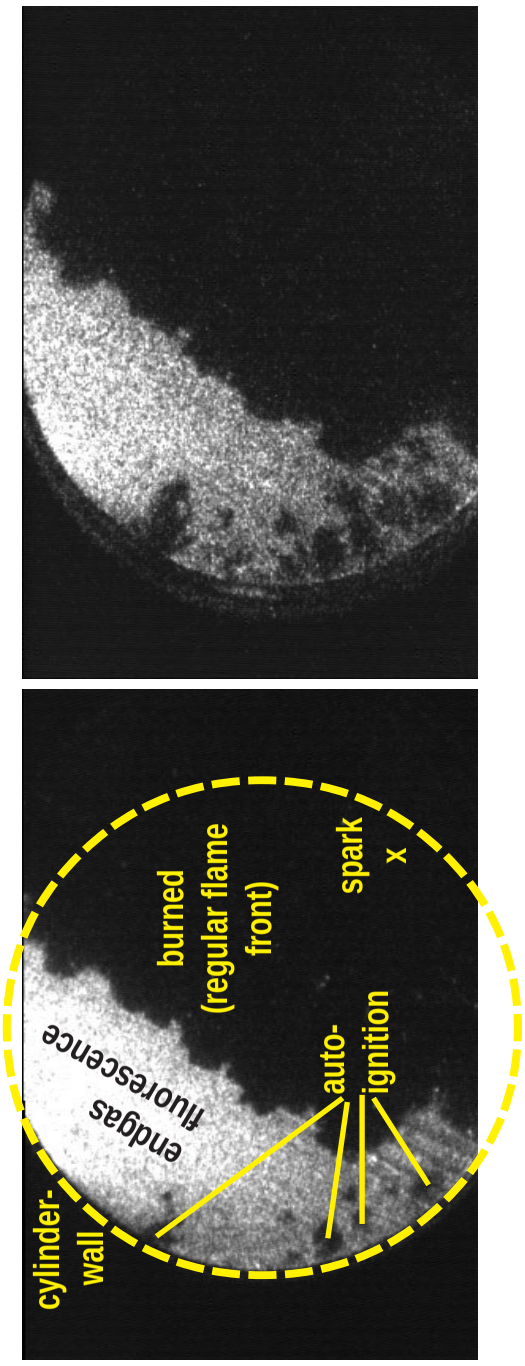
spark
x
burned
(regular flame
front)
auto-
ignition
endgas
fluorescence
cylinder-
wall

Fig. 4.

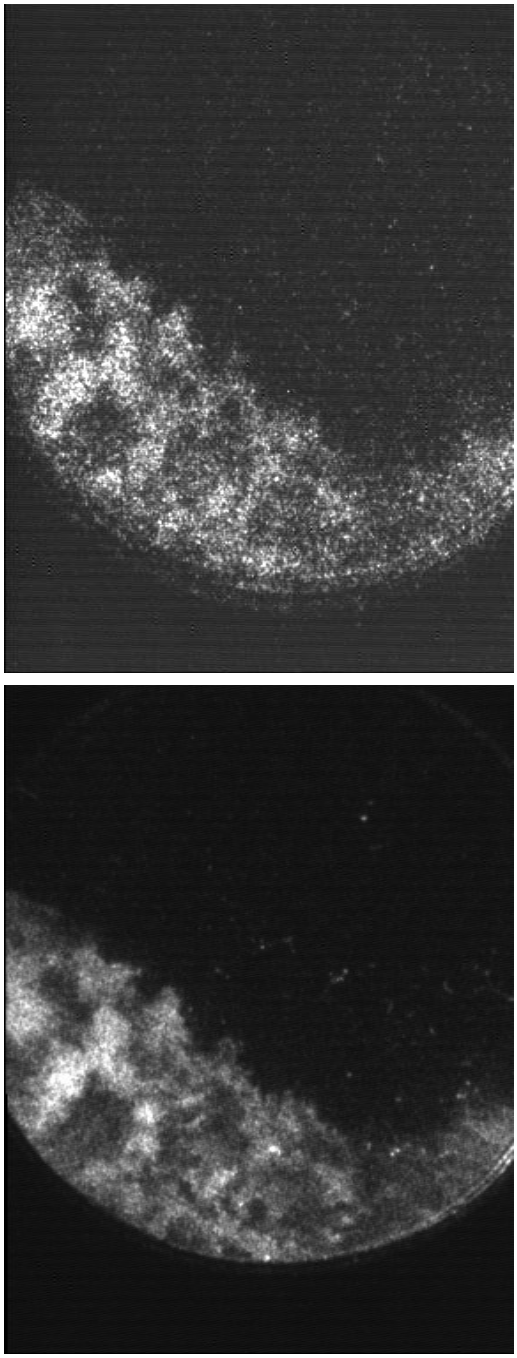

Fig. 5.

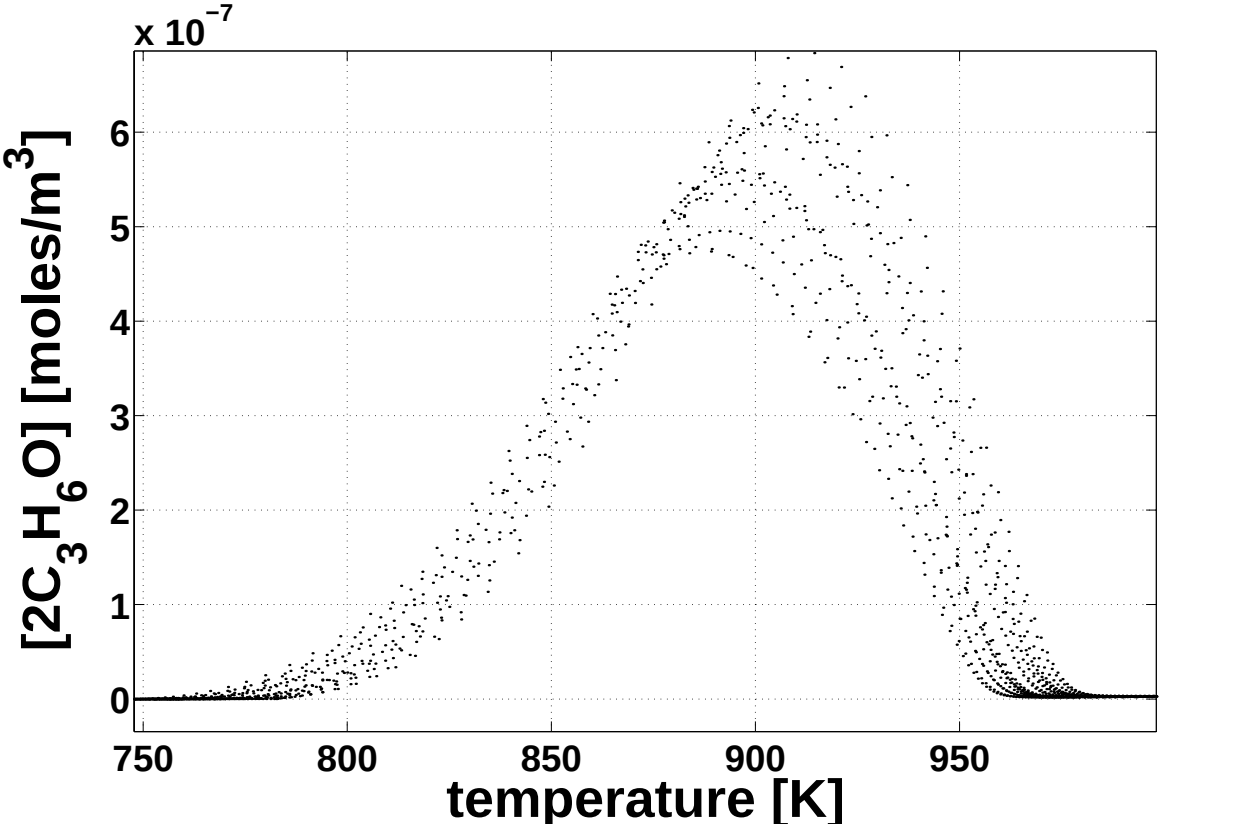
x 10^−7
[2C3H6O] [moles/m3]
0
1
2
3
4
5
6
750
800
850
900
950
temperature [K]

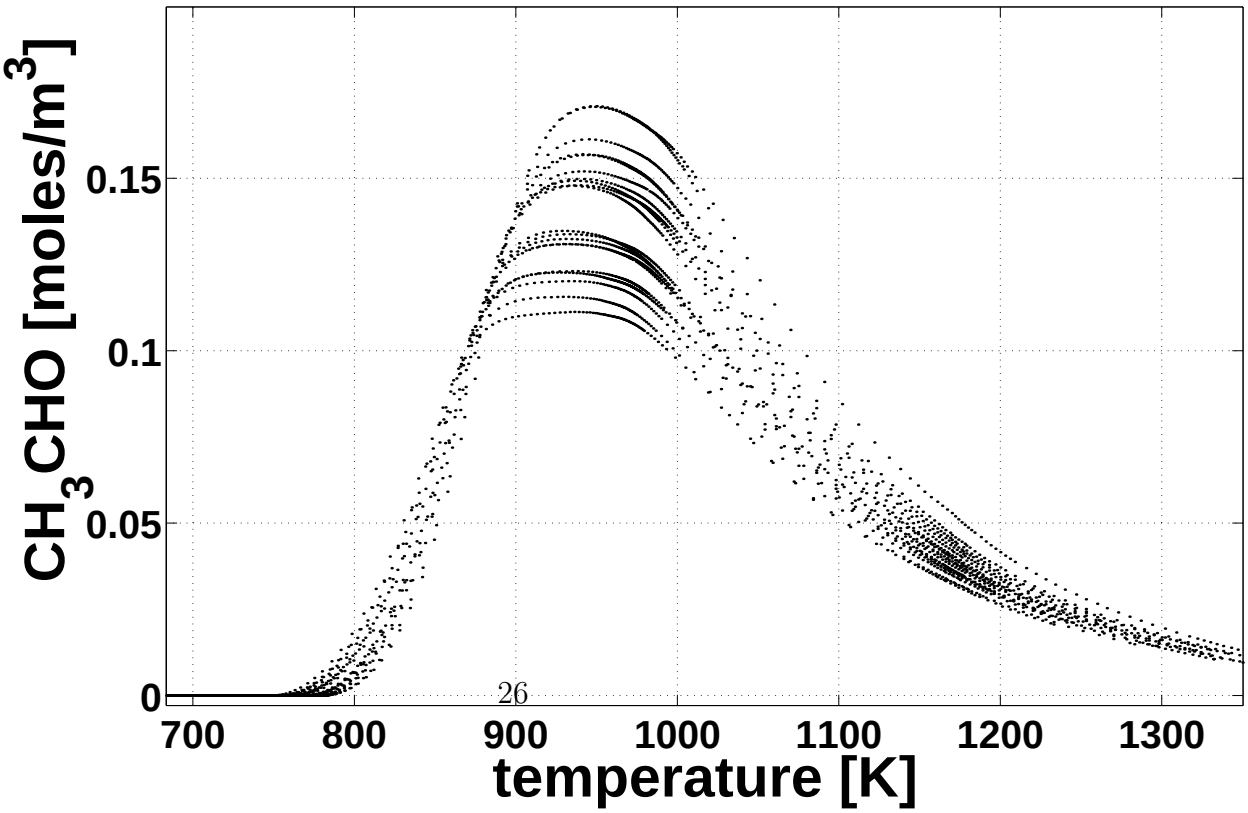
CH3CHO [moles/m3]
0
0.05
0.1
0.15
700
800
900
1000
1100
1200
1300
temperature [K]

Fig. 6.

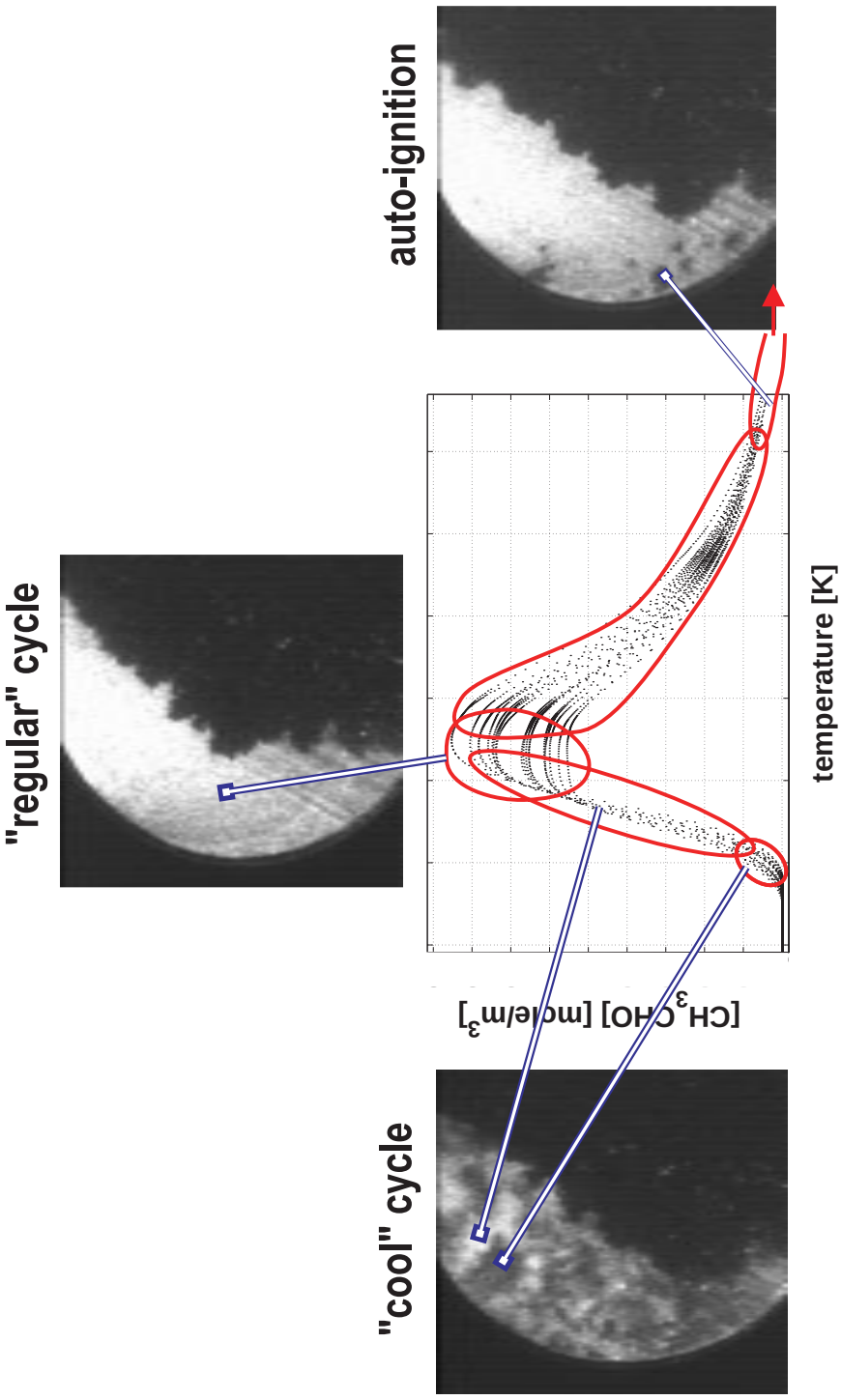
auto-ignition
"regular" cycle
"cool" cycle
temperature [K]
[CH3CHO] [mole/m3]

Fig. 7.

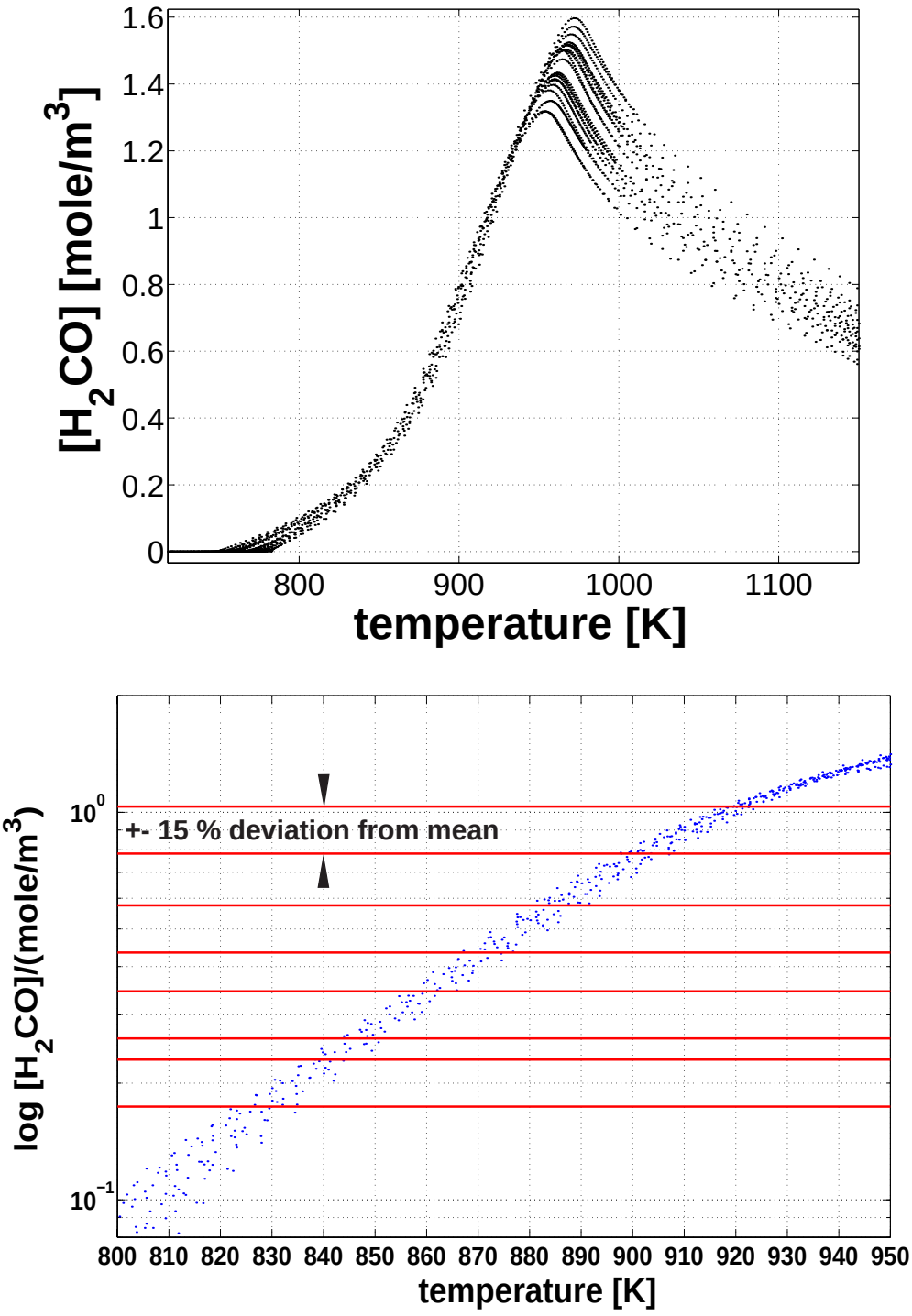
1.6
1.4
1.2
1
0.8
0.6
0.4
0.2
0
[H2CO] [mole/m3]
800
900
1000
1100
temperature [K]
+- 15 % deviation from mean
10^0
10^-1
log [H2CO]/(mole/m3)
800 810 820 830 840 850 860 870 880 890 900 910 920 930 940 950
temperature [K]

Fig. 8.

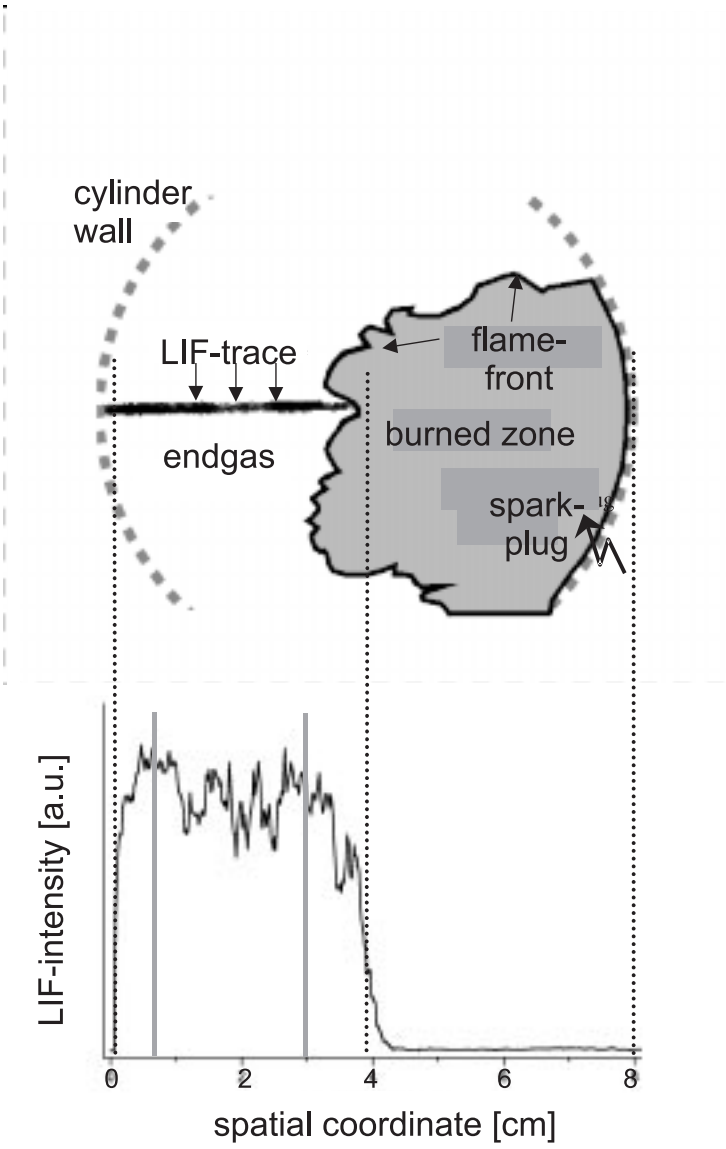
cylinder
wall
LIF-trace
flame-
front
burned zone
endgas
spark-
plug
LIF-intensity [a.u.]
0
2
4
6
8
spatial coordinate [cm]